PAPER

CrossMark
← click for updates

Structural and magnetic studies of perovskite YCr$_{0.5}$Mn$_{0.5}$O$_3$

Hannah James,[a] Brendan J. Kennedy,*[a] Thomas A. Whittle[a] and Maxim Avdeev[b]

The structure of YCr$_{0.5}$Mn$_{0.5}$O$_6$, established from Rietveld refinement of powder neutron diffraction data, contains Cr and Mn that are disordered on the octahedral sites. The structure is best described in the orthorhombic space group *Pbnm*. Low temperature neutron diffraction data reveal a G-type antiferromagnetic type arrangement, with a ferromagnetic component along the *b*-axis, indicating that the Cr and Mn couple ferro (or possibly ferri) magnetically to each other.

Introduction

The complex interplay between the spin, orbit, lattice and charge degrees of freedom in doped manganese perovskites results in examples of unique and fascinating phenomena, including colossal magnetoresistance, magnetocaloric response and multiferroic behaviour.[1] Orbital ordering in Mn^{3+} perovskites is a consequence of a Jahn–Teller type distortion,[2] that is also evident in Cu^{2+} (3d^9) perovskites, where it is related to the observed superconducting behaviour.

The title oxide Y$_2$CrMnO$_6$ has recently become of interest, however the structure of this is not well established. Liu and co-workers[3] described it as having an orthorhombic structure in space group *Pnma* (an alternate setting of *Pbnm*) where the Cr^{3+} and Mn^{3+} cations are disordered on the octahedral sites. If the two cations are disordered it is best to describe this as YCr$_{0.5}$Mn$_{0.5}$O$_3$ to emphasise the disorder. Independently Hao and co-workers[4,5] argued that the Cr^{3+} and Mn^{3+} cations were ordered, suggesting two monoclinic structures initially in *P*2$_1$/*n* but later revising this to *P*2$_1$/*b*. The cation ordered arrangement is best represented by the formula Y$_2$CrMnO$_6$. These two monoclinic structures differ in the arrangement of the Cr^{3+} and Mn^{3+} cations, the former having a rock-salt like ordering whereas the latter has a layered ordered arrangement. Both Liu[3] and Hao[4,5] relied on X-ray diffraction to establish the structure of YCr$_{0.5}$Mn$_{0.5}$O$_3$. The applicability of this approach is questionable since the electron configuration of Cr^{3+} and Mn^{3+} differ by a single electron; consequently Cr^{3+} and Mn^{3+} are practically indistinguishable when investigated using conventional X-ray diffraction methods.

Ordering of cations in perovskites typically requires a significant difference in the ionic size and/or charge of the cations[6] as illustrated in Sr$_2$NiWO$_6$.[7] Charge ordering occurs in oxides such as Ba$_2$Bi^{III}Bi^{V}O$_6$.[8] Orbital ordering can also occur leading to a lowering of symmetry as illustrated in the vanadates AVO$_3$.[9] Cation ordering, irrespective of its origin, is often associated with unusual electronic properties[10] and the ferrimagnetism reported for YCr$_{0.5}$Mn$_{0.5}$O$_3$ may provide evidence of this. Whilst there are numerous examples of cation ordering in perovskite-type oxides,[6] ordering of Cr^{3+} and Mn^{3+} in a perovskite would be exceptional, given the similarity in the size and charge of these two cations and would be a unique example of orbital effects inducing chemical ordering. Given the absence of any well know examples of such ordering there is a need to establish if such ordering does indeed occur.

In the present paper we have utilised powder neutron diffraction to establish a precise and accurate structure of YCr$_{0.5}$Mn$_{0.5}$O$_3$. Whilst the X-ray scattering factors of Cr^{3+} and Mn^{3+} are extremely similar the neutron scattering lengths are dramatically different; Mn has a coherent scattering factor of −3.73 fm and Cr has a coherent scattering factor of 3.635 fm. The magnetic structure of YCr$_{0.5}$Mn$_{0.5}$O$_3$ has also been investigated.

Experimental

A 5 g sample of YCr$_{0.5}$Mn$_{0.5}$O$_3$ was prepared by the solid state synthesis of Y$_2$O$_3$, Cr$_2$O$_3$ and Mn$_2$O$_3$. After drying the oxides, stoichiometric quantities of Y$_2$O$_3$, Cr$_2$O$_3$ and Mn$_2$O$_3$ were mixed in an agate mortar and pestle under acetone. The resulting mixture was transferred to an alumina boat and then heated overnight in air at 1173 K, and then, after regrinding, at 1473 K for 24 hours using a muffle furnace. The powder was reground, pressed into pellets at heated at 1673 K for 96 hours with periodically re-grounding and pelleting until the powder

[a]School of Chemistry, The University of Sydney, Sydney, NSW 2006, Australia. E-mail: Brendan.Kennedy@sydney.edu.au
[b]Australian Nuclear Science and Technology Organisation, Lucas Heights, NSW 2234, Australia

X-ray diffraction pattern no longer changed. The sample was cooled to room temperature in the furnace over a period of ~5 hours. The final product was black.

Magnetic measurements were conducted between 4 K and 300 K under both field cooled and zero field cooled conditions with a measuring magnetic field of 1 kOe using a Quantum Design Physical Properties Measurement System. Magnetic hysteresis loops were measured at 5 K.

X-ray diffraction data were collected on a PANalytical X'Pert Pro MPD X-ray diffractometer (45 kV, 40 mA). Data were collected for a 2θ range of 5 to 120° using $Cu_{K\alpha}$ radiation. Neutron powder diffraction data were measured using the high resolution powder diffractometer Echidna at ANSTO's OPAL facility at Lucas Heights using wavelengths of 1.622 or 2.439 Å.[11]

Results and discussion

A polycrystalline sample of $YCr_{0.5}Mn_{0.5}O_3$ was prepared as described by Hao et al.[4] The extent of cation disorder in perovskites can be influenced by the highest temperature used to prepare the sample and the rate of cooling, with rapid cooling tending to stabilise disordered structures. The present sample was heated to 1673 K, the same maximum temperature employed by Hao et al.,[4] and the sample was slowly cooled. The structure of this was initially investigated using powder X-ray diffraction (XRD) data. As described by Liu et al.[3] and Hao et al.[4] Rietveld refinement assuming a disordered arrangement of the Cr and Mn cations in the orthorhombic Pbnm space group was successful. Examination of the data revealed a weak peak near $2\theta = 30°$ that was identified as coming from the presence of a small amount of Y_2O_3, Liu et al. noted that high pressure was required to eliminate the formation of this phase.[3] Models in the two monoclinic models described by Hao et al. ($P2_1/n$ and $P2_1/b$)[4,5] were also tested and these gave comparable quality fits to the XRD data, reflecting the similarity in the X-ray scattering factors of Cr^{3+} and Mn^{3+}. The same cannot be said for the neutron powder diffraction (NPD) data. Fig. 1 illustrates a portion of the powder neutron diffraction pattern for $YCr_{0.5}Mn_{0.5}O_3$ recorded at room temperature.

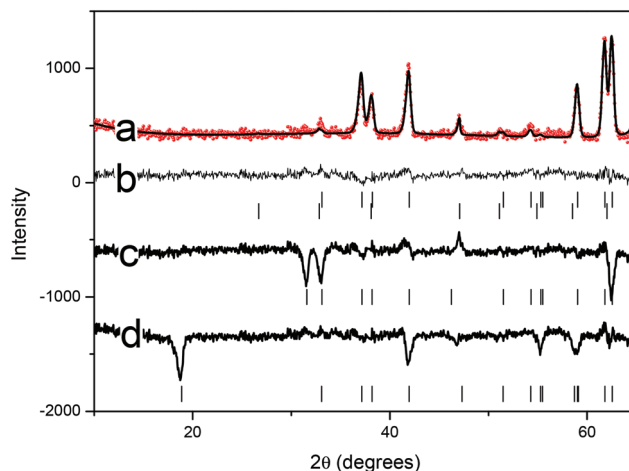**Fig. 1** Portion of the neutron diffraction pattern recorded for $YCr_{0.5}Mn_{0.5}O_3$ at room temperature using $\lambda = 2.44$ Å neutrons. The top trace (a) is the observed data (symbols) and the fit (solid line) to this in the orthorhombic space group Pbnm. Below this trace (b) is the difference between the observed and calculated profiles in (a) and the tick markers for the (upper) orthorhombic phase and (lower) Y_2O_3 phases. Trace (c) is the difference between the observed data and the best fit in $P2_1/n$, and immediately below are the tick marks showing the positions of the Bragg reflections in $P2_1/n$. Trace (d) is the difference between the observed data and the best fit in $P2_1/b$, and immediately below are the tick marks showing the positions of the Bragg reflections in $P2_1/b$. Although the fits using the monoclinic models allowed for the presence of trace amounts of Y_2O_3 the tick marks for this phase are not shown below traces (c) and (d) for clarity.

The models for the $P2_1/b$ and $P2_1/n$ symmetries both calculate significant intensity in peaks when there is none present, making it clear that they are not appropriate. Conversely the fit obtained using the disordered model in Pbnm contains no significant discrepancies. It should be noted that in the refinement of the Pbnm model the atomic displacement parameter of the disordered Cr/Mn site was fixed at 0.5×10^{-2} Å^3. The 1 : 1 mixture of Cr and Mn gives this site an effective neutron scattering length of close to zero.

The refined structural parameters, obtained using a combination of the 1.62 and 2.44 Å neutron data sets are summarised in Table 1, whilst the fit to the 1.62 Å pattern is shown in Fig. 2. The unit cell parameters in the orthorhombic Pbnm

Table 1 Refined structural parameters for $YCr_{0.5}Mn_{0.5}O_3$ using neutron diffraction data. $a = 5.25074(8)$ $b = 5.62780(10)$ $c = 7.47670(10)$ Å. Volume = 220.937(6) Å^3. $R_p = 5.40$ $R_{wp} = 4.16$ and $\chi^2 = 2.08$

Name	x	y	z	Ui/Ue × 100		
Y	0.01702(20)	0.57255(19)	0.25	0.860(27)		
Cr	0	0	0	0.5[a]		
Mn	0	0	0	0.5[a]		
O1	−0.10690(24)	−0.03501(25)	0.25	0.79[b]		
O2	0.19654(18)	0.31212(20)	0.05396(13)	1.02[b]		
	U^{11}	U^{22}	U^{33}	U^{12}	U^{13}	U^{23}
O1	0.89(8)	1.16(8)	0.32(7)	0.67(6)	0	0
O2	0.52(4)	1.83(6)	0.71(5)	−0.15(4)	0.08(5)	0.02(5)

[a] Fixed at 0.5×10^{-2}. [b] Anisotropic displacement parameters were employed for the oxygen atoms, whilst that of the disordered Cr/Mn cations was fixed.
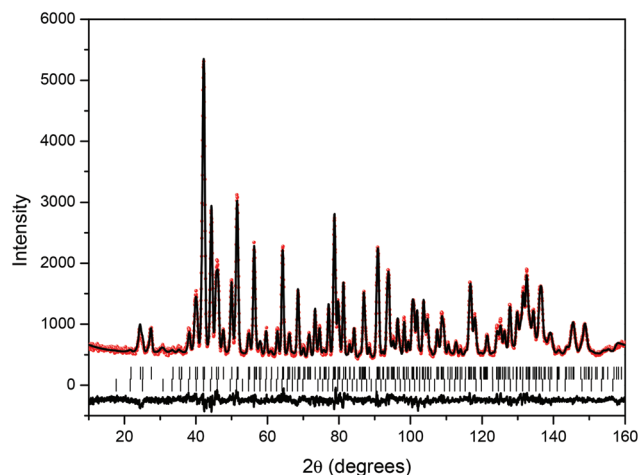
Fig. 2 Observed calculated and difference neutron diffraction profiles for $YCr_{0.5}Mn_{0.5}O_3$ at room temperature using $\lambda = 1.62$ Å neutrons. The structure was refined in the orthorhombic space group *Pbnm*. The lower set of tick marks are from Y_2O_3.
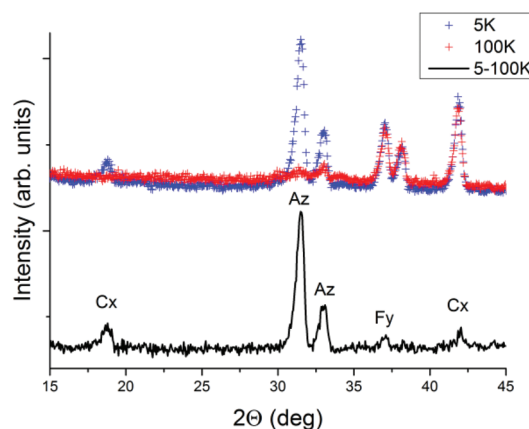

Fig. 4 Neutron powder diffraction data collected at 5 K and 100 K and the difference (blue and red symbols and black solid line, respectively). The letters indicate magnetic peaks associated with a particular magnetic ordering mode in the CxFyAz model.

model are related to the unit cell length of the ideal cubic perovskite a_0 as $a \sim \sqrt{2}a_0 b \sim \sqrt{2}a_0 c \sim 2a_0$ with the expansion in the cell being a consequence of cooperative tilting of the corner sharing $(MnCr)O_6$ octahedra. The tilting in *Pbnm* is described as $a^- a^- c^+$ in Glazer's nomenclature. The coordination of the $(MnCr)O_6$ octahedra is highly distorted with four short and two long $(MnCr)$–O bonds $(MnCr)$–O(1) 1.9616(4)Å and $(MnCr)$–O(2) 1.9544(10) and 2.0768(11)Å. This reflects the presence of a Jahn–Teller like distortion associated with the Mn^{3+} cation. That both the Mn and Cr cations are trivalent was verified by Bond Valence calculations that gave a BVS of 3.19 for Mn and 2.90 for Cr. The distortion of the $(MnCr)O_6$ octahedra is associated with the large pseudo-tetragonal distortion of the unit cell with $\sqrt{2}b/c = 1.06$, This is smaller than the distortion in $YMnO_3$, 1.11,[12] that only contains Mn^{3+} but is larger than that seen in the Mn^{4+} perovskite $CaMnO_3$ $b/c = 1.00$ [13] or the Cr^{3+} containing oxide $YCrO_3$ $b/c = 1.04$.[14] A similar large distortion of both the BO_6 octahedra and cell metric was observed in Sr_2MnSbO_6 where extensive disorder of the Mn^{3+} and Sb^{5+} cations occurs.[15]

Magnetic measurements of $YCr_{0.5}Mn_{0.5}O_3$ reveal a divergence of the zero field cooled and field cooled susceptibilities near 75 K as observed previously. Above 150 K the inverse susceptibilities display Curie–Weiss type behaviour with an effective magnetic moment of $\mu_{eff} = 4.12\mu_\beta$ with a negative Weiss constant of $\theta = -57$ K indicative of an antiferromagnetic ground state, although the rapid increase in the field cooled susceptibility is suggestive of ferrimagnetism. The observed magnetic moment and Weiss constant are in excellent agreement with the results described by Liu *et al.* ($4.53\mu_\beta$ and -59 K respectively) and the moment is close to the value expected for a 1 : 1 mixture of Cr^{3+} (d^3) and Mn^{3+} (d^4), $4.39\mu_\beta$. The magnetization (M) *vs.* applied magnetic field (H) measurements at 4 K showed clear hysteresis loops, depicting ferrimagnetic behaviour.

An unusual feature of Fig. 3 is the crossover from positive to negative values during the ZFC measurements. As locally d^4_{HS}–d^4_{HS}, d^4_{HS}–d^3, and d^3–d^3 pairs are expected to couple *via* superexchange ferro-, ferro-, and antiferromagnetically, respectively, this is believed to be a consequence of magnetic compensation between the Mn^{3+}–Mn^{3+} and Mn^{3+}–Cr^{3+} contact

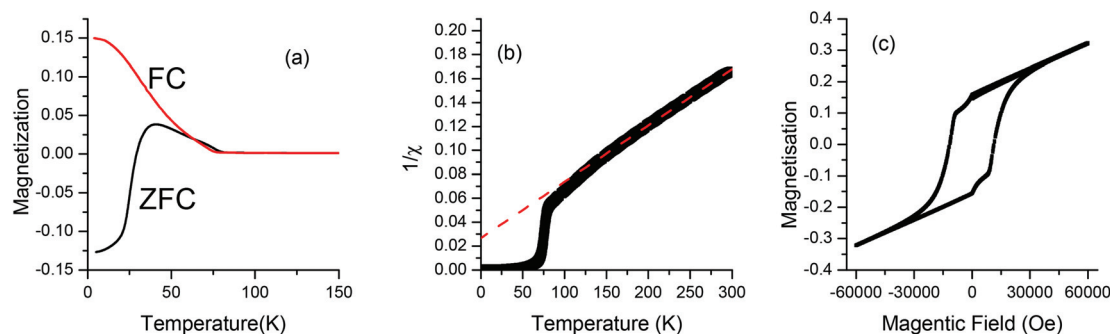
Fig. 3 (a) Temperature dependence of the field-cooled (FC) and zero-field-cooled (ZFC) magnetization of $YMn_{0.5}Cr_{0.5}O_3$ was measured at magnetic field of 1 kOe. (b) Temperature dependence of the inverse (FC) molar magnetic susceptibility. The dashed line is a linear fit to the high temperature region. (c) Magnetization as a function of applied magnetic field for $YMn_{0.5}Cr_{0.5}O_3$ at 5 K.

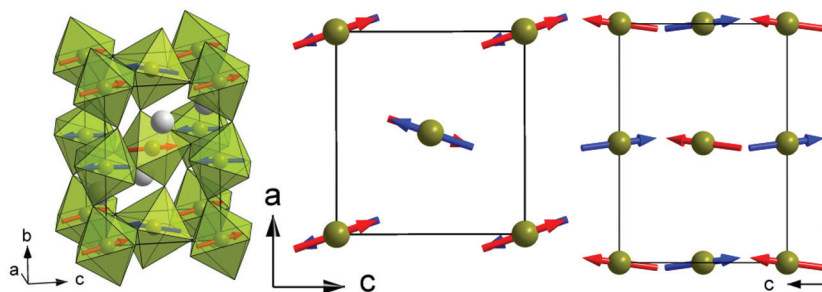**Fig. 5** General view of the crystal and magnetic structure of Y(Cr$_{0.5}$Mn$_{0.5}$)O$_3$ (left) and projections along b- (middle) and a-axes (right) (in *Pnma* setting).

rich domains with the moment aligned antiparallel to each other. We note that the effect of compensation was not observed by Liu[3] as it is clearly highly dependent on the sample preparation protocol determining Mn and Cr distribution uniformity over the sample.

Neutron diffraction measurements at low temperatures showed the presence of magnetic scattering, Fig. 4. All the magnetic peaks were indexed by a chemical unit cell *i.e.* with the propagation vector k(0,0,0). Representational analysis performed with BasiReps for the (4a) Wyckoff site of the space group 62 in the standard *Pnma* setting revealed AxGyCz, GxAyFz, CxFyAz, and FxCyGz possible ordering models (irreducible represenations Γ1, Γ3, Γ5, and Γ7, respectively). Data examination showed that the best magnetic model is unambiguously Γ5 CxFyAz. The structure is best described as G-type, where the AFM component is along c-axis, containing a small ferromagnetic component along the b-axis, see Fig. 5.

In the modelling of the magnetic site it was assumed that the reduction of the moment from the full moment of $S = 3/2$ Cr^{3+} and $S = 2$ Mn^{3+} is the same for both cations. The final Rietveld plot is shown in Fig. 6. The determined components of magnetic moment along a-, b-, and c-axes are 0.63(3), 0.25(14), 1.83(2)μ_B, respectively yielding the total moment of 1.95(3)μ_B which is ~0.65 of the full moment. The moment reduction is not surprising as locally some Mn^{3+} and Cr^{3+} atoms will have a combination of the nearest magnetic neighbours with interactions of varying strength or even type (AFM/FM).

Finally, the model indeed allows ferromagnetic component (along b-axis) and then we have two options: either Cr and Mn are coupled ferro- or ferri- to each other. The data does not allow these options to be distinguished. That such coupling can exist in the disordered model was overlooked by Hiu *et al.*[4,5]
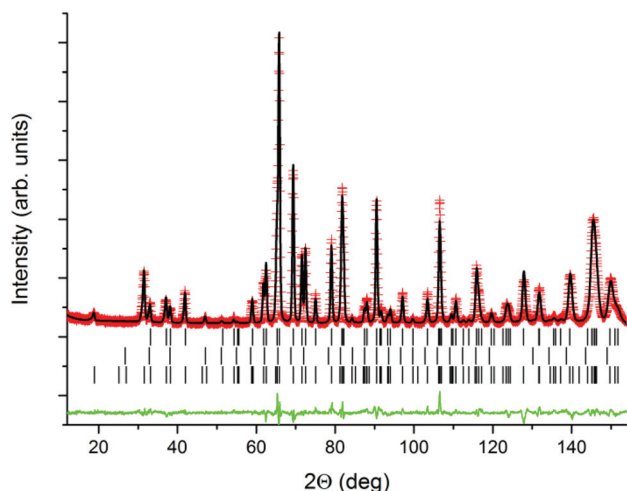
Conclusions

Neutron diffraction measurements show that the structure of the perovskite YCr$_{0.5}$Mn$_{0.5}$O$_6$ is adequately described in the orthorhombic space group *Pbnm*, in which the Cr^{3+} and Mn^{3+} cations randomly occupy the octahedral sites. Whilst it is possible altering the conditions used to prepare the sample can alter the degree of disorder, the neutron data demonstrate that the previous suggestion of ordering of the Cr^{3+} and Mn^{3+} cations is incorrect. Magnetic susceptibility measurements confirm the presence of magnetic ordering. Low temperature neutron diffraction data reveal that the strongest magnetic exchange is indicative of a G-type antiferromagnetic type arrangement. These data reveal the presence of a ferromagnetic component along the b-axis, indicating that the Cr and Mn couple ferro (or possibly ferri) magnetically to each other.

Fig. 6 The Rietveld plot for Y(Cr$_{0.5}$Mn$_{0.5}$)O$_3$ refined against NPD data collected at 5 K. The red crosses and black and green solid lines indicate the observed and calculated patterns and their difference, respectively. The tick marks from top to bottom indicate the position of the diffraction peaks of the nuclear structures of Y(Cr$_{0.5}$Mn$_{0.5}$)O$_3$, Y$_2$O$_3$ (0.53(5)wt.%), and magnetic structure of Y(Cr$_{0.5}$Mn$_{0.5}$)O$_3$. R_p = 4.53%, R_{wp} = 5.93%, R_{mag} = 6.14%, χ^2 = 3.10.

Acknowledgements

References

1 J. M. D. Coey, M. Viret and S. von Molnar, *Adv. Phys.*, 1999, **48**, 167–293.

2 Z. Popovic and S. Satpathy, *Phys. Rev. Lett.*, 2002, **88**, 197201.

3 F. Y. Liu, J. J. Li, Q. L. Li, Y. Wang, X. D. Zhao, Y. J. Hua, C. T. Wang and X. Y. Liu, *Dalton Trans.*, 2014, **43**, 1691–1698.

4 L. Yang, Q. Y. Duanmu, L. Hao, Z. F. Zhang, X. P. Wang, Y. Y. Wei and H. Zhu, *J. Alloys Compd.*, 2013, **570**, 41–45.

5 L. Hao, L. Yang, M. H. Lee, T. H. Lin, Z. F. Zhang, X. N. Xie and H. Zhu, *J. Alloys Compd.*, 2014, **601**, 14–18.

6 M. T. Anderson, K. B. Greenwood, G. A. Taylor and K. R. Poeppelmeier, *Prog. Solid State Chem.*, 1993, **22**, 197–233.

7 Q. D. Zhou, B. J. Kennedy, C. J. Howard, M. M. Elcombe and A. J. Studer, *Chem. Mater.*, 2005, **17**, 5357–5365.

8 B. J. Kennedy, C. J. Howard, K. S. Knight, Z. M. Zhang and Q. D. Zhou, *Acta Crystallogr., Sect. B: Struct. Sci.*, 2006, **62**, 537–546.

9 S. Miyasaka, Y. Okimoto, M. Iwama and Y. Tokura, *Phys. Rev. B: Condens. Matter*, 2003, **68**, 100406.

10 K. L. Kobayashi, T. Kimura, H. Sawada, K. Terakura and Y. Tokura, *Nature*, 1998, **395**, 677–680.

11 K. D. Liss, B. Hunter, M. Hagen, T. Noakes and S. Kennedy, *Physica B*, 2006, **385–86**, 1010–1012.

12 J. A. Alonso, M. J. Martinez-Lope, M. T. Casais and M. T. Fernandez-Diaz, *Inorg. Chem.*, 2000, **39**, 917–923.

13 Q. D. Zhou and B. J. Kennedy, *J. Phys. Chem. Solids*, 2006, **67**, 1595–1598.

14 K. Sardar, M. R. Lees, R. J. Kashtiban, J. Sloan and R. I. Walton, *Chem. Mater.*, 2011, **23**, 48–56.

15 M. Cheah, P. J. Saines and B. J. Kennedy, *J. Solid State Chem.*, 2006, **179**, 1775–1781.